Adaptive Kalman Filter Based Data Aggregation in Fault-Resilient Underwater Sensor Networks

Lauri Vihman and Jaan Raik
Department of Computer Systems, Taltech, Estonia
lauri.vihman@taltech.ee, jaan.raik@taltech.ee

***Abstract*—Sensor Networks in harsh underwater environments are prone to faults and anomalies that may lead to deteriorated data quality or even failures. This paper proposes a fault-resilient underwater sensor network based on sensor data aggregation by updating the measurement error matrix of an adaptive Kalman filter, where the error matrix is updated using adjusted measured value difference from the predicted value as well as the age of the latest measurement (i.e. latency). A case study on a real-world harbor water flow monitoring use-case shows the advantages of the proposed method. The experiments indicate that the adaptive and difference based Kalman filter aggregation provides for a significantly smoother aggregation in case of high fault rates in sensors' readings when compared to traditional Kalman filter and median value based aggregation techniques.**

I. Introduction

Data Aggregation methods are widely used to conserve energy and communication bandwidth in sensor networks [1]–[5]. When sensor nodes have limited energy, it is reasonable not to send all the data to the receiving sink. Data aggregation is referred as amongst the most important energy-saving analysis processes [3]. In recent years, research has been done on aggregation methods that are best applicable for underwater environments [1], [2]. In addition, aggregation techniques have been used to address security concerns (compromised nodes), data integrity and redundancy as well as the lifetime of sensor networks [4].

Methods of data aggregation for network communication can be distinguished by structure - flat methods, where all the sensors are playing the same role, clustering-based, tree-based and hybrid methods [2] and by functional approach like aggregation by feedback control, quantile digest, distributed source coding [5].

The Kalman Filter (KF) is one of the most popular mathematical state estimation tools [6] that includes multiple variants and is extensively used in robotics [7]–[11] and combined to fuzzy logic [9], [10] and sensor fusion [7], [9]–[13] techniques.

An Extended Kalman Filter has been applied to estimate gas leaks in pipelines [6] and to overcome signal noise as well as limitations of different kinds of sensors [12].

For sensor data aggregation, Kalman Filters have been used as a security tool to detect false data injection attacks in sensor networks [14] and also for noise elimination from signals with ordered weight averaging [15] and in wireless sensor networks to achieve a distributed consensus [16].

979-8-3503-3959-8/23/$31.00 ©2023 IEEE

While above-mentioned works on Kalman Filters did not address hardware faults, the following works focus also on that aspect. A generic detection and compensation of occurrence of transient and permanent faults was described [13] using Kalman Filter and correspondingly registering T_{Fault} and P_{Fault} variables, respectively, when values were exceeding a defined threshold. However, it relied on a difference between measured and predicted values compared to a defined threshold and did not consider signal latency nor sensor outage. Kalman filter based fault diagnosis and accommodation has been studied in [8] limited to robot wheel actuators and optical encoders. A more recent study using a Kalman Filter for robot localization can overcome faults including sensor outage and data corruption of IMU sensors [11]. However, no sensor signal latency is considered and the prediction weights are linear.

While previous works have applied Kalman filters in fault-tolerant applications to the best of the authors' knowing this is the first work to propose a KF that includes different uncertainty sources and applies the adaptive KF based data aggregation in USNs.

Contributions of this work are as follows:

- Incorporating different sources of sensor uncertainty by including the time series measurements' difference and age/latency uncertainty for adapting a KF to compensate incorrect readings for avmore efficient state prediction.
- Proposing nonlinear, parabolic and sigmoid, sensor uncertainty functions from the residual difference for the latency and difference based Adaptive Kalman techniques, respectively.
- Applying and evaluating the proposed adaptive KF based data aggregation techniques in a harbor Underwater Sensor Network (USN) with extremely unreliable sensor readings.

II. Underwater Sensor Network Application

In this Section, we introduce the layered data architecture and installation of the sensor network in the application scenario of a harbor monitoring use case.

A. Sensor Network Installation

The underwater sensor network considered in this paper is for monitoring sea currents in the harbor. The Sensor Nodes $S = \{s_i\}$ of the network are installed to the harbor infrastructure to notify approaching ships about the water

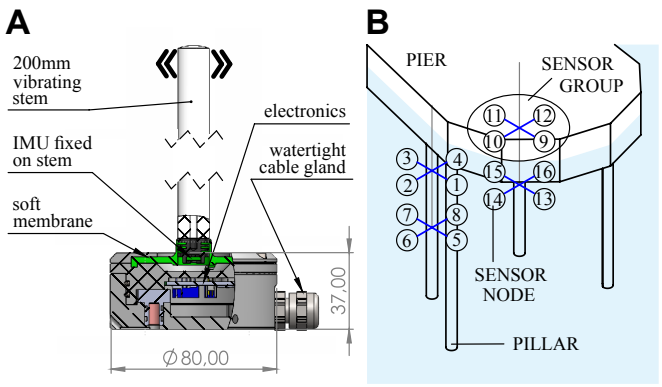

Fig. 1. A) Sensor Node B) Harbor Installation

flow around the piers. The goal is that berthing ships get information about the flow and turbulence from Sensor Nodes installed on the pillars of the pier. The Sensor Nodes are connected to the Sensor Gateway with underwater cables over RS-485 serial communication, thus the configuration of the underwater sensor network is fixed.

The Sensor Node applied in the case study is shown in Figure 1.A and its detailed description is given in [17]. The Sensor Nodes measure the flow magnitude and direction from the stem vibrating in the flow. An IMU (Inertial Measurement Unit) embedded into the Sensor Node calculates the accelerations of the stem in x and y directions. In the current implementation, to estimate the flow magnitude from the IMU data, a 15s series of IMU raw data is transformed with FFT (Fast Fourier Transform) into a frequency domain in 120s intervals and the PSD (Power Spectral Density) is used to find the flow magnitude using calibrations described in [17]. All the Sensor Nodes are wired to the Sensor Gateway in a star network topology.

The Sensor Nodes $\{s_i\}$ are installed around the pillars at two different depths so that at both depths 4 Sensor Nodes are attached around the pillar at 90 degrees angle from each other forming a logical Sensor Group $G = \{g_j\}$. This is necessary because depending on the direction of the flow, the pillar itself always obstructs some of the Sensors Nodes from the flow. Therefore each aggregation of 4 Sensor Nodes (Sensor Group) is used to estimate the flow at each point.

In total the installation has 16 Sensor Nodes, grouped into 4 aggregations (Sensor Groups) of 4 sensors each as shown in Figure 1.B.

B. Layered data model implementation

Table I presents the data-driven layers of the sensor network architecture. There are three data layers - raw, processed and aggregated that correspond to different functionalities that can be loosely mapped to IoT layers as shown in Table I.

At the **Raw data layer** is data that is measured and transferred by the set of Sensor Nodes $S = \{s_i\}$. The Sensor Nodes measure and send values periodically and the event of receiving a valid test packet at the Raw Data Layer by

TABLE I
DATA LAYERS AND THEIR MAPPING TO IOT LAYERS

Data Layer	State	IoT Layers
Raw	direct data from sensors	Edge
Processed	pre-processed data from sensors	Edge/Fog
Aggregated	data combined to sensor groups	Cloud

sensor s_i at a discrete time instance t is $\rho(i,t)$. The raw measurement value $\rho(i,t)$ of the sensor node s_i at time t is a vector containing values such as Inertial Measurement Unit's XYZ positions, temperature and pressure.

All the valid $\rho(i,t)$ measurement values received during a time interval T, containing n time instances, are pushed into the raw data queue of length n, which acts as a First-In-First-Out (FIFO) data buffer $F = \{f_1, f_2, ..., f_n\}$, where $f_1, ..., f_n$ represent n latest valid $\rho(i,t)$ measurement values. There is a separate queue F_i for each sensor node s_i.

Processed data layer is used to obtain the processed data. At the predefined time intervals the data in F are processed by a signal processing function Ψ to obtain the processed data value of $\sigma(i,t)$, i.e. $\sigma(i,t) = \Psi(F)$

Initially Ψ transforms the raw values $\rho(i,t)$ from F_i into an intermediate processed values $\sigma'(i,t)$. $\sigma'(i,t)$ contains values that are in a linear relation to quantities required by the end user.

Next, the processing function Ψ converts values from $\sigma'(i,t)$, using predefined calibration and offset constants that are specific for the installation and concrete sensor instance, to quantities required by the end user of the harbor water flow monitoring application (e.g. velocity).

Aggregated data is generated for the Sensor Groups $G = \{g_j\}$ from the processed data σ of the Sensor Nodes $\{s_i\}$. The purpose of the aggregation process is to provide transition from single Sensor Nodes' data to Sensor Groups' data. Subsequently, the aggregated value $\alpha(j,t)$ of the sensor group g_j at Aggregated data layer is calculated by an aggregation function Ω on converted values $\sigma(i,t)$ of the sensor nodes s_i that belong to the sensor group g_j, i.e. $\alpha(j,t) = \Omega(\{\sigma(i,t)|s_i \in g_j\})$.

III. FAULT-RESILIENT DATA AGGREGATION

In the current Section, we propose an implementation of the data aggregation function Ω introduced in the previous section. Input values for the aggregation function are the processed values $\sigma(i,t)$ and output values are $\alpha(j,t)$, respectively.

A. Adaptive Kalman filter for data aggregation

Kalman Filter (KF) is a widely used technique for data analysis, such as filtering, smoothing, initialization, forecasting, assimilation and aggregation [18]. In our case, due to physical limitations, harsh underwater environment and possibility of occurrence of both, persistent and intermittent faults, the sensors vary from correct measurements. To cope with that issue, we rely on a Sensor Group g_j (see II-B) to generate data fusion for univariate measurements - that is multiple sensors simultaneously measure similar physical entity. We are

applying KF in the Aggregation Data layer (see II-B) after an initial signal processing is done.

We are using adaptive KF for data fusion to compute aggregated data and get the filtered estimate that is more reliable than the sources. Sensor values are read and transformed to velocity values simultaneously after a predefined constant time interval. To calculate aggregated values of the 4-sensor groups, adaptive KF is used. The KF is implemented as follows:

$$
\begin{aligned}
X_{t|t-1} &= AX_{t-1|t-1} \\
V_t &= Y_t - X_{t|t-1}H \\
P_{t|t-1} &= AP_{t-1|t-1}A^T + Q \\
S_t &= HP_{t|t-1}H^T + R_t \\
K_t &= P_{t|t-1}H^T S_t^{-1} \\
X_{t|t} &= X_{t|t-1} + K_t V_t \\
P_{t|t} &= P_{t|t-1} - K_t S_t K_t^T
\end{aligned}
$$

where $t \in N$ is discrete time, $Y \in \mathbb{R}^4$ is the measurement vector containing σ_i values of the current sensor group, $X \in \mathbb{R}$ is the state estimate scalar, $Q \in \mathbb{R}$ is process noise scalar constant, $H \in \mathbb{R}^4$ is the observation vector constant, $V \in \mathbb{R}^4$ is the calculated innovation residual vector, $A \in \mathbb{R}$ is state matrix constant, $P \in \mathbb{R}$ is the updated estimate covariance scalar, $R \in \mathbb{R}^{4\times4}$ is the sensor uncertainty co-variance matrix, $S \in \mathbb{R}^{4\times4}$ is the innovation co-variance matrix and $K \in \mathbb{R}^4$ is the Kalman gain vector.

The sensor uncertainty covariance matrix R is updated using L_i and D_i weights (see III-B) in different configurations as explained next.

In case of *Kalman Static*, sensor uncertainty R is not updated during the filter's execution.

In case of *Kalman Difference* aggregation, sensor uncertainty matrix R is set to $n(D_i) \times J_4$, where J_4 is the unit matrix and n is the normalization function explained in III-B.

In case of *Kalman Latency* aggregation, sensor uncertainty R is set to $n(L_i) \times J_4$.

In case of *Kalman Adaptive* aggregation, sensor uncertainty R is set to $(n(L_i) + n(D_i)) \times J_4$.

The output value of the aggregation function Ω, i.e. α_j of the sensor group g_j at time t receives its value from $X_{t|t}$.

The calculation is iterative over time t and for aggregation, the values X_t are used. To make KF adaptive, the covariance matrix R_t is externally updated increasing sensors' uncertainties with increasing difference from aggregated X_t value and measurement latency, indicating outliers and probable sensor faults.

B. Uncertainty from the difference of measurement and estimation

When detecting outlier values based on the difference between estimation and measurement, we argue that this should not be linear - small differences in velocity should be proportionally more tolerated than larger differences. The uncertainty value based on the difference does not have to have an upper limit, since the type of the sensors used that have a defined measurement range - frequencies beyond this range are not reported and thus cannot affect the uncertainty value of the sensor. For adaptive weights we applied the following function $D_i = c(\sigma(i) - x)^2$, where $\sigma(i)$ is the processed value of the sensor s_i, x is the predicted value of KF, thus $\sigma(i) - x$ is the residual, and c is a constant 1.5 that was chosen empirically. The normalized graph of the function is shown in Figure 2 right.

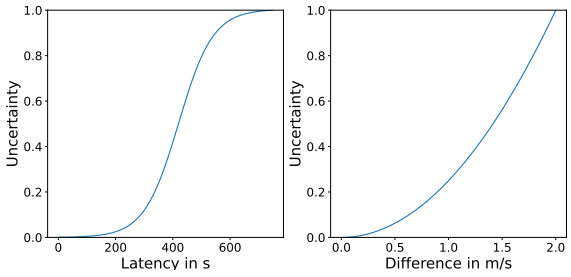

Fig. 2. Normalized sensor uncertainty from measurement and prediction difference (residual) and the latest measurement latency

For uncertainty caused by measurement latency we applied the following sigmoid function. $L_i = \frac{1}{1+e^{\frac{-t_i}{m}+h}}$, where m = 60 and h = 7 and t_i is the latency of the latest valid measurement of the i-th sensor s_i in seconds. Normalized uncertainty values based on latency are presented in Figure 2 left.

The normalization is performed to be able to compare the uncertainty function values and give them weights to calculate the sensor uncertainty co-variance matrix using the following normalization function $n(v) = \frac{v-min(V)}{max(V)-min(V)}$, where v is a value from a vector of values V to be normalized.

IV. Experiments

Experiments in two different underwater environments were conducted. The Flow Obstuction experiment was a short time experiment that took place in freshwater in a river on February 2, 2023. For this experiment, in addition to the hydromast sensors, ADV (Acoustic Doppler Velocimeter) measurements were also used as reference values. The sensor network was installed to a river bed (See IV-A) and the water flow was manually disturbed and interfered.

The Harbor Experiment was a long-time experiment active from April to August 2020. The sensor network was installed into sea water by a harbor for measuring underwater currents (See II-A). For this experiment we did not have a reference device. The sensors were not disturbed nor interfered manually, the collected data was naturally occurring. Most of the time during that period the water flow was too slow to be measurable with sensors due to non-windy weather conditions. However, there were a couple of time intervals with a stronger water movement.

A. Flow obstruction experiment

The hydromast sensors were attached on a metal bar at 20cm intervals. Perpendicular to the centre of the hydromast was another bar with attached ADV (Acoustic Doppler Velocimeter, Nortek Vectrino Profiler) approximately 50cm from the hydromast metal bar. The construction was installed to a river bottom around 1m depth with the ADV facing the flow and hydromasts side by side behind it. The order of the hydromasts from the shore was H24, H25, H26, H27. The unobstructed water velocity appeared similar at all hydromasts. The hydromast offset coefficients are calibrated after installation to correspond to ADV beams mean value magnitude. The velocity is calculated using the magnitude of median x and y axis angles of 1 sec time frame of 50hz measurements.

Figure 3 shows the obstruction experiment.

- Sensor measurements are shown as dots. Aggregate different Kalman filters are shown as lines.
- A human was obstructing the flow by standing in the water for every hydromast for 30 sec in the following order - 1st H24, 2nd H25, 3rd H26, 4th H27
- It can be seen that the obstruction changed the hydromast angles correspondingly as the dots representing single measurements move downwards at specific times.
- H25 obstruction is less clear, but happened also while obstructing H24 and H26, thus standing near the 1st and 3rd hydromast obstructed the flow also at the 2nd hydromast.

It can also be seen from Fig. 3 that the sensors' water flow measurement is consistent and adequately reacts to changes in the water flow. From the Figure, it can be seen that Kalman difference is the most optimal aggregation method for this case, as it is accurately filtering out disturbances at individual sensors. It was followed by median and Kalman adaptive aggregation. However, Kalman latency and Kalman static were far more tolerant to disturbances at individual sensors.

B. Harbor experiment

Finally an experiment was carried out on naturally occurring data from the actual use case. From the data collected during the five-month period we selected an interval on May 7th, 2020 where all of the sensors in the sensor group were active and there was enough flow to measure velocity and direction. The flow is in a measurable range from approximately 6:30 to 20:00 when it begins to fade. The day is characteristic for representing the harshness of the environment as there are multiple gaps and outliers in the readings and one of the sensors (H3) stops providing new measurements around 13:20.

In this harsh, real-world environment Kalman difference and Kalman adaptive are performing equally efficiently, while the aggregation provided by Median and Kalman latency methods is far too unstable. The weakest performance is obtained by Kalman static that is consistently overestimating the water current flow.

As the result of the experiments, the most robust and stable aggregation performance was achieved by the Kalman

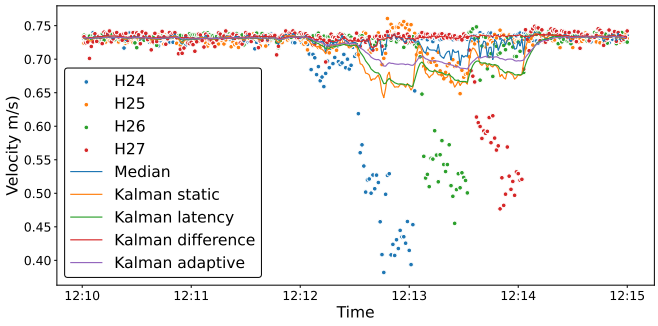

Fig. 3. Comparison of the aggregation methods in the obstruction experiment

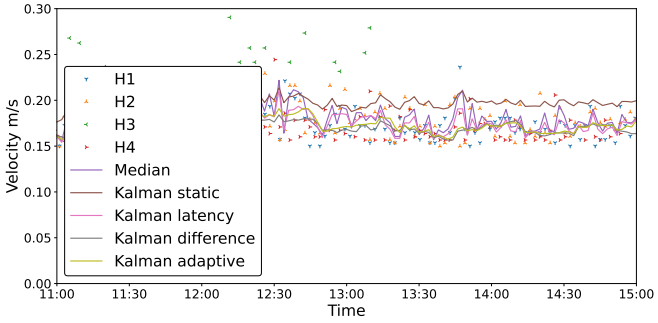

Fig. 4. Aggregation methods and processed values for velocity measurement in the harbor experiment

difference method that took into account the difference of the measurement value at the sensor from the estimated value. This method performed well in a stable current as well as in case of disturbances and also in very harsh conditions, where there were gaps and outliers.

Kalman adaptive was slightly less accurate with faulty sensor reading but became more robust and equal to Kalman difference in case of more frequent gaps in readings. It might become the preferred option when conditions are extremely harsh and become even more dominated by gaps.

V. Conclusion

A fault-resilient underwater sensor network based on sensor data aggregation by updating the measurement error matrix of an adaptive Kalman filter was proposed. A case study on a real-world harbor water flow monitoring use-case showed that the adaptive and difference based technique allowed for a significantly smoother aggregation in case of high fault rates in sensors' readings when compared to traditional Kalman filter and median value based aggregation techniques.

Acknowledgment

This work has received funding from the European Commission's Horizon 2020 Research and Innovation programme under grant agreement No 101037643 and by Estonian Centre of Research Excellence EXCITE.

REFERENCES

[1] N. Goyal, M. Dave, and A. K. Verma, "Data aggregation in underwater wireless sensor network: Recent approaches and issues," *J. King Saud Univ. - Comput. Inf. Sci.*, vol. 31, pp. 275–286, jul 2019.

[2] S. Abbasian Dehkordi, K. Farajzadeh, J. Rezazadeh, R. Farahbakhsh, K. Sandrasegaran, and M. Abbasian Dehkordi, "A survey on data aggregation techniques in IoT sensor networks," *Wirel. Networks*, vol. 26, no. 2, pp. 1243–1263, 2020.

[3] S. A. Abdulzahra and A. K. M. Al-Qurabat, "Data Aggregation Mechanisms in Wireless Sensor Networks of IoT: A Survey," *Int. J. Comput. Digit. Syst.*, vol. 13, pp. 1–15, jan 2023.

[4] K. Gulati, R. S. Kumar Boddu, D. Kapila, S. L. Bangare, N. Chandnani, and G. Saravanan, "A review paper on wireless sensor network techniques in Internet of Things (IoT)," *Mater. Today Proc.*, vol. 51, pp. 161–165, 2022.

[5] E. Fasolo, M. Rossi, J. Widmer, and M. Zorzi, "In-network aggregation techniques for wireless sensor networks: a survey," *IEEE Wirel. Commun.*, vol. 14, pp. 70–87, apr 2007.

[6] R. Doshmanziari, H. Khaloozadeh, and A. Nikoofard, "Gas pipeline leakage detection based on sensor fusion under model-based fault detection framework," *J. Pet. Sci. Eng.*, vol. 184, no. July 2019, 2020.

[7] T. Huang, H. Jiang, Z. Zou, L. Ye, and K. Song, "An integrated adaptive Kalman filter for high-speed UAVs," *Appl. Sci.*, vol. 9, no. 9, 2019.

[8] S. Mellah, G. Graton, E. M. E. Adell, M. Ouladsine, and A. Planchais, "Mobile robot additive fault diagnosis and accommodation," *2019 8th Int. Conf. Syst. Control. ICSC 2019*, pp. 241–246, 2019.

[9] J. Z. Sasiadek and P. Hartana, "Sensor data fusion using Kalman filter," *Proc. 3rd Int. Conf. Inf. Fusion, FUSION 2000*, vol. 2, pp. 19–25, 2000.

[10] P. J. Escamilla-Ambrosio and N. Mort, "Hybrid Kalman Filter-Fuzzy Logic Adaptive Multisensor Data Fusion Architectures," *Proc. IEEE Conf. Decis. Control*, vol. 5, no. December, pp. 5215–5220, 2003.

[11] M. Kheirandish, E. A. Yazdi, H. Mohammadi, and M. Mohammadi, "A fault-tolerant sensor fusion in mobile robots using multiple model Kalman filters," *Rob. Auton. Syst.*, vol. 161, 2023.

[12] E. Foxlin, "Inertial head-tracker sensor fusion by a complementary separate-bias Kalman filter," *Proc. - Virtual Real. Annu. Int. Symp.*, pp. 185–194, 1996.

[13] P. J. Escamilla-Ambrosio and N. Mort, "Multi-sensor data fusion architecture based on adaptive Kalman filters and fuzzy logic performance assessment," *Proc. 5th Int. Conf. Inf. Fusion, FUSION 2002*, vol. 2, no. 3, pp. 1542–1549, 2002.

[14] K. Miao, W. A. Zhang, and X. Qiu, "An adaptive unscented Kalman filter approach to secure state estimation for wireless sensor networks," *Asian J. Control*, vol. 25, no. 1, pp. 629–636, 2023.

[15] M. H. Basiri, N. L. Azad, and S. Fischmeister, "Distributed time-varying kalman filter design and estimation over wireless sensor networks using OWA sensor fusion technique," *2020 28th Mediterr. Conf. Control Autom. MED 2020*, pp. 325–330, 2020.

[16] J. Qin, J. Wang, L. Shi, and Y. Kang, "Randomized Consensus-Based Distributed Kalman Filtering over Wireless Sensor Networks," *IEEE Trans. Automat. Contr.*, vol. 66, no. 8, pp. 3794–3801, 2021.

[17] A. Ristolainen, J. A. Tuhtan, and M. Kruusmaa, "Continuous, near-bed current velocity estimation using pressure and inertial sensing," *IEEE Sens. J.*, vol. PP, no. c, pp. 1–1, 2019.

[18] J. Durbin and S. J. Koopman, *Time Series Analysis by State Space Methods*. Oxford University Press, may 2012.